Nuclear Reactor Theory

Lesson 9: The Critical Reactor IV

Additional Modeling and Analysis Considerations…

Prof. John R. White
Chemical and Nuclear Engineering
UMass-Lowell, Lowell MA

Lesson 9 Objectives

Explain the basic concepts of spatial and resonance self shielding.

Explain qualitatively how lumping of the fuel into a heterogeneous geometry affects the thermal utilization and resonance escape probability.

Explain, in general terms, how to create equivalent homogeneous regions that properly account for the heterogeneous detail in real geometries .

Explain briefly the nonlinear coupling that exists between the core physics problem and the temperature and flow distributions within a reactor.

Define and compute the total, axial, and radial power peaking factors in various reactor geometries.

Lesson 9 Objectives (cont.)

Explain the existence of the peak in the thermal flux that is usually observed just beyond the core-reflector interface in most thermal systems.

Explain the observed behavior in both the fast and thermal flux profiles in and near control rod locations in a typical thermal system.

Explain, based on the fuel assembly design and core configuration, some of the fine structure in the observed flux profiles within the UMLRR.

Heterogeneous Effects

We have consistently used the term "homogeneous" to describe the material properties in all our previous models.

Clearly, however, most reactor geometries are not simple homogeneous mixtures of fuel, moderator/coolant, structure, and control.

Instead, the actual geometries are quite complicated and quite heterogeneous -- with discrete regions of fuel, clad, coolant, structure, etc. (e.g. see the sketch of a typical Westinghouse PWR 17×17 fuel assembly).

So how do we deal with this???

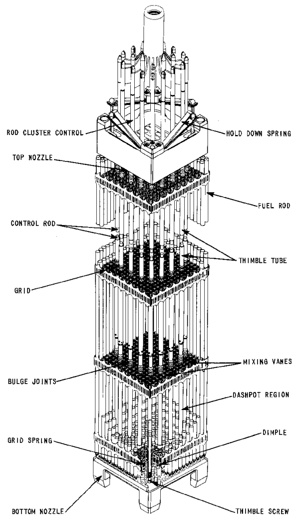

Heterogeneous Effects (cont.)

The challenge here is "How do we create equivalent homogeneous regions that properly account for the heterogeneous detail?".

This task is treated as part of the cross section averaging and collapsing process that we briefly discussed in the Fundamentals of NSE course.

The equation used for collapsing the fine group data for some spatial region z is of the form

$$\sigma_{gz} = \frac{\frac{1}{N_z}\sum_{g'\in g}\int_{v_z} N(\vec{r})\sigma_{g'}(\vec{r})\phi_{g'}(\vec{r})d\vec{r}}{\sum_{g'\in g}\int_{v_z}\phi_{g'}(\vec{r})d\vec{r}}$$

where g' = fine group number, g = broad group index, $\vec{r}$ = spatial variable, and z = zone of interest.

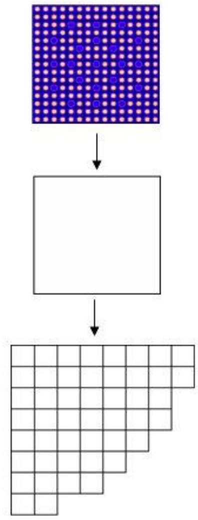

Heterogeneous Effects (cont.)

To evaluate this equation, one needs to know the

- geometry -- the spatial variable and domain of interest v_z
- material composition -- $N(\vec{r})$ and its average value over v_z
- spatial variation of the fine group weight function $\phi_{g'}(\vec{r})$.

This typically requires that a fine group 1-D or 2-D model be employed to solve for $\phi_{g'}(\vec{r})$.

To do this, some representative portion of the overall heterogeneous geometry is modeled in 1-D or 2-D geometry.

This unit cell or unit assembly calculation is designed to be simple enough so that $\phi_{g'}(\vec{r})$ can be computed, but accurate enough so that the resultant average cross sections are indicative of a full multidimensional heterogeneous geometry fine group analysis.

Heterogeneous Effects (cont.)

The broad-group cell or assembly averaged cross sections can then be used in full or partial core 2-D and 3-D computer models that only incorporate homogeneous regions within the models.

The two key issues involved here relate to the concepts of space and energy self shielding.

These two concepts are illustrated nicely in the two sketches: one shows the depression in the thermal flux that often occurs in the vicinity of a fuel rod (or other absorber material), and the other shows the flux depression that can occur in the neighborhood of a resonance.

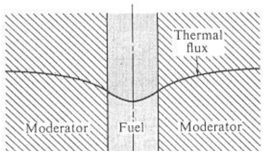

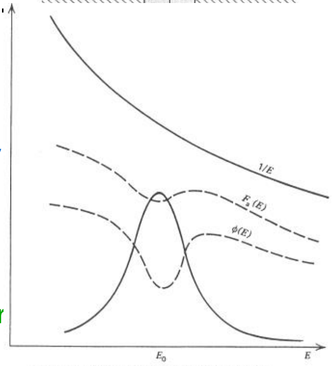

Flux depression in the neighborhood of a resonance.

Heterogeneous Effects (cont.)

These examples indicate the fine detail that must be treated in the space and energy dependent weight function, $\phi_{g'}(\vec{r})$, when collapsing to the problem-dependent broad group level.

These effects are treated in a formal way in sophisticated cross section processing codes (e.g. SCALE, CASMO, WIMS, APPOLO, SERPENT, etc.) -- but the details will not be treated here!

One can also address the subject of heterogeneous systems, in a qualitative fashion, with focus on how the components of the 6-factor formula change for heterogeneous versus homogenous systems.

The two factors mostly affected are the thermal utilization, f, and the resonance escape probability, p.

$$f = \frac{\langle \Sigma_{a2}^{F}\phi_2 \rangle}{\langle \Sigma_{a2}\phi_2 \rangle} \quad \text{and} \quad p = \frac{\langle \Sigma_{1\to 2}\phi_1 \rangle}{\langle \Sigma_{a1}\phi_1 \rangle + \langle \Sigma_{1\to 2}\phi_1 \rangle}$$

Heterogeneous Effects (cont.)

Within this context, lumping of the fuel tends to reduce the thermal flux in the fuel region (spatial self shielding) and this tends to decrease the thermal absorption rate in the fuel -- thus $f_{het} < f_{homo}$.

Concerning the resonance region, lumping of the fuel also increases the atom density and macroscopic absorption cross sections in the fuel resonances.

This, in turn, can cause a flux dip at the localized resonance energies (resonance self shielding) and this tends to decrease resonance absorption and increase the resonance escape probability -- thus $p_{het} > p_{homo}$.

In most low enriched systems, since the absorption cross section within some of the key resonances is greater than at thermal, the lumping of the fuel generally increases p more than it decreases f.

Heterogeneous Effects (cont.)

Thus, $(pf)_{het} > (pf)_{homo}$ for low enriched systems and

$$k_{het} > k_{homo} \quad \text{(for low enriched systems)}$$

However, it should be noted that the effects on f and p (and the other factors within the 6-factor formula) are quite subtle, and detailed computer modeling is usually needed to quantify these effects for real design and analysis purposes.

In the SCALE system:

The BONAMI and CENTRM/PMC modules treat the resonance self shielding.

The XSDRN (1-D) and NEWT (2-D) modules treat the spatial self shielding.

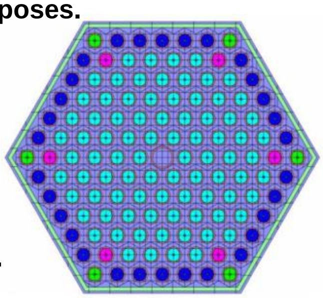

Grid structure and material placement for VVER-440 model.

Coupled Thermal Hydraulics & Physics

Before any reactor physics computations can occur, we must have knowledge of the material composition and temperature, so that the appropriate atom densities and macroscopic cross sections can be determined.

However, in practice, the computed flux distribution and power density profile affect the material temperature and density distribution which, in turn, impacts the physics calculation, which then affects the temperature profile, etc. etc.

This coupling represents a nonlinear relationship, since the cross sections are implicitly related to the computed flux and power distribution.

In addition, since the temperatures and densities are spatially dependent, the macroscopic cross sections are also functions of space (fuel burnup also causes a strong spatial dependence).

Coupled Thermal Hydraulics & Physics

This spatial behavior and nonlinear coupling is definitely important in high power systems, and this is usually treated within a nonlinear iteration scheme within the design codes used within the nuclear industry.

The energy removal process will be discussed in some detail and some actual heat transfer calculations will be performed at a later point in your NE program studies.

Knowledge of these subjects will allow us to estimate the fuel and coolant temperature profiles in an operating PWR and BWR, in research reactors, etc..

However, at this point, it is sufficient to note that the connection between the physics calculations and the thermal-hydraulic computations is the power density, $PD(\vec{r})$.

Coupled Thermal Hydraulics & Physics

Recall that the power density is given by

$$PD(\vec{r}) = \kappa \sum_g \Sigma_{fg}(\vec{r})\phi_g(\vec{r})$$

Note also that, in the heat transfer literature, the internal heat generation term is often given as q''' -- so, in nuclear heat transport studies, $q'''(\vec{r}) = PD(\vec{r})$ for the configuration under study (with usual units of W/cm^3 or BTU/ft^3).

Thus, the physics calculation feeds the thermal-hydraulic analysis and the resultant temperature profile allows us to compute the appropriate macroscopic cross sections for the system -- and this nonlinear iteration scheme is continued until the power density and temperature profiles no longer change…

Coupled Thermal Hydraulics & Physics

Within this context, it should also be noted that the physics analysis also feeds any safety calculations that will be performed for a given reactor system.

In safety analyses, we are often interested in the worse case scenario, so usually the hottest channel is the focus of the analysis.

For a hot channel analysis, we are interested in the fuel pin and channel configuration with the maximum power production, since this often leads to the highest temperatures and the greatest potential for fuel damage -- and excessive temperatures that can lead to fuel damage must be avoided under all possible scenarios.

Power Peaking Factors

The total power peaking factor, F, the radial peaking factor, F_R, and the axial shape function are the usual quantities that are passed along from the physics analysis team to the safety analysis group.

These values allow easy computation of the overall peak power density and/or the power density profile in the hot pin.

In particular, the total peaking factor is a ratio of the peak to average power density, or

$$F = \frac{PD_{max}}{PD_{ave}}$$

and the radial peaking factor is given by

$$F_R = \frac{\text{maximum pin power}}{\text{average pin power}}$$

Power Peaking Factors (cont.)

These two quantities are clearly related by the axial peaking factor, F_z, which represents the peak to average power density along the hot fuel pin.

In particular, we have $F = F_R F_z$

These peaking factors are important because, with these quantities, one can easily construct the peak heat generation rates within the hot channel, where

$$\text{max power density} = F \times PD_{ave} = F\left(\frac{P}{V_{fuel}}\right)$$

and

$$\begin{array}{c}\text{power produced}\\ \text{in hot pin}\end{array} = F_R \times \text{ave pin power} = F_R\left(\frac{P}{\#\text{ of fuel pins}}\right)$$

where P is the total reactor power and V_{fuel} is the total volume of all the fuel pins.

Power Peaking Factors (cont.)

Since the average power density and the average pin power are readily available quantities, if F and F_R are known, then the above expressions can be easily evaluated for these two important quantities -- that is, the maximum power density in the system and the power (or average power density) produced in the hottest fuel pin in the reactor.

In general, F, F_R, and F_z are determined from detailed physics calculations for the system -- and this is usually done via numerical solution and appropriate manipulation of the resultant discrete power density distribution.

However, if the core geometry is simple enough to allow analytical calculations, then these quantities can be determined from simple integration of the analytical results.

As an example, let's consider the finite bare homogeneous cylindrical reactor model studied previously -- see next slide...

Peaking Factors: Bare Cylindrical Reactor

In this 1-group case, the resultant power density is given by

$$PD(r,z) = \kappa\Sigma_f \phi(r,z)$$

and the total reactor power is simply the integral of this expression over the full core volume, or

$$P = \int \kappa\Sigma_f \phi d\vec{r} = \kappa\Sigma_f \int \phi(r,z) 2\pi r dr dz$$

where

$$\phi(r,z) = AJ_0\left(\frac{2.4048}{R} r\right)\cos\left(\frac{\pi}{H} z\right)$$

Clearly the maximum PD occurs at the center of the reactor (at r = 0 and z = 0), so that PD_{max} is simply

$$PD_{max} = \kappa\Sigma_f A = \kappa\Sigma_f \left(\frac{2.4048\pi}{4J_1(2.4048)} \frac{P}{\kappa\Sigma_f V_{fuel}}\right) = \frac{3.638P}{V_{fuel}}$$

This assumes a small extrapolation distance (see Lesson 7)

Peaking Factors: Bare Cylindrical Reactor

Now, since the total peaking factor is simply a ratio of the peak to average power density, we have

$$F = \frac{PD_{max}}{PD_{ave}} = \frac{3.638P/V_{fuel}}{P/V_{fuel}} = 3.638$$

Also, since the peak in the core radial profile occurs at r = 0, the axial power density profile at this radial location is given by

$$PD(0,z) = \kappa\Sigma_f \phi(r,z)\big|_{r=0} = \kappa\Sigma_f A\cos\left(\frac{\pi}{H}z\right) = C\cos\left(\frac{\pi}{H}z\right)$$

and the axial peaking factor is given by

$$F_z = \frac{PD(0,z)\big|_{max}}{PD(0,z)\big|_{ave}} = \frac{C}{\frac{C}{H_o}\int_{-H_o/2}^{H_o/2}\cos\frac{\pi z}{H}dz} = \frac{C}{\frac{C}{H_o}\frac{2H}{\pi}\sin\frac{\pi H_o}{2H}} \approx \frac{\pi}{2} = 1.571$$

Peaking Factors: Bare Cylindrical Reactor

Doing the same type of analysis for the radial peaking factor at z = 0, gives

$$PD(r,0) = \kappa\Sigma_f \phi(r,z)\big|_{z=0} = \kappa\Sigma_f A J_0\left(\frac{2.4048}{R}r\right) = CJ_0\left(\frac{2.4048}{R}r\right)$$

and

Again, see Lesson 7 for the details of the integrations done here.

$$F_R = \frac{PD(r,0)\big|_{max}}{PD(r,0)\big|_{ave}} = \frac{C}{\frac{2\pi C}{\pi R_o^2}\int_0^{R_o} r\,J_0\left(\frac{2.4048r}{R}\right)dr}$$

$$= \frac{C}{\frac{2\pi C}{\pi R_o^2}\frac{R_o R}{2.4048}J_1\left(\frac{2.4048R_o}{R}\right)} \approx \frac{2.4048}{2J_1(2.4048)} = 2.316$$

Peaking Factors: Bare Cylindrical Reactor

These results are indeed consistent with the above discussion, since

$$F = F_R F_z = (2.316)(1.571) = 3.638$$

The various peaking factors defined here are extremely important in reactor design and safety analysis studies, and these will be seen again when the subject of nuclear heat transport is discussed later in the NE curriculum.

For now, we emphasize that computing these quantities is one of the primary goals (among several others) of the reactor physics analysis, and they represent the primary link between the reactor physics and thermal hydraulics groups within many nuclear design organizations.

Some Modeling Results

All our analytical results to date have been restricted to simple reactor geometries.

However, before completing our introduction to steady state reactor theory, we should show some typical results for a few more realistic reactor geometries.

Thus, to close out this Lesson, we will discuss two different reactor models:

IAEA PWR Benchmark and UMass-Lowell Research Reactor

The examples to follow used either the VENTURE and/or DORT codes:

VENTURE uses diffusion theory and allows 1-D, 2-D, or 3-D modeling

DORT uses transport theory in 2-D configurations

Some Modeling Results

The VENTURE models usually focus on computing the multiplication factor, rod worth distributions, and other reactivity-related parameters, as well as determining the few-group flux and power distributions in the system.

For the 2-D DORT analyses, we typically use a coupled 47-group neutron and 20-group gamma cross section library so that we can determine the multigroup neutron and gamma radiation fields throughout the system (including the excore regions).

Often, the VENTURE and DORT codes are used in tandem to support a particular study -- where VENTURE is used to generate the fission source within the core, and then DORT is used to transport the fission neutrons into the regions outside the core (see discussion of the FNI later in this Lesson).

VENTURE: $(L-\lambda F)\phi = 0$ and DORT: $L\phi = \lambda F\phi = Q$

IAEA PWR Benchmark

This benchmark model was used extensively in the 1980s and early 1990s to validate a lot of the computational methods development that was being done at that time.

The formal specifications are for a full 1/8-core symmetric 3-D system but, for illustration here, we only address the 2-D XY planar region at the axial centerline of the system.

Here we include a model without control as well as the reference 2-D mid-core model with control inserted within the four assemblies as implied in the sketch.

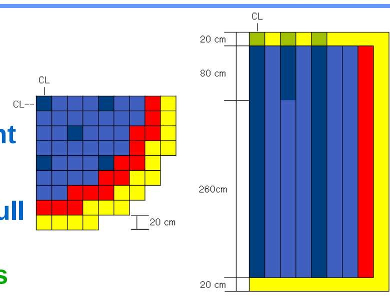

Core Geometry

Two Group Cross Sections for Each Composition

Material	D_g	Σ_{ag}	$\nu\Sigma_{fg}$	$\Sigma_{s2\leftarrow1}$
Fuel1	1,500	0,010	0,000	0,020
	0,400	0,085	0,135	
Fuel1+Rod	1,500	0,010	0,000	0,020
	0,400	0,130	0,135	
Fuel2	1,500	0,010	0,000	0,020
	0,400	0,080	0,135	
Reflector	2,000	0,000	0,000	0,040
	0,300	0,010	0,000	
Reflector+Rod	2,000	0,000	0,000	0,040
	0,300	0,055	0,000	

IAEA PWR Benchmark (cont.)

The **two primary goals** of this simulation are:

1. To illustrate the **peak in the thermal flux** that is observed **just beyond the core-reflector interface** in most thermal systems, and

2. To show the observed **behavior of the fast and thermal flux profiles in and near control rod locations** in a thermal system.

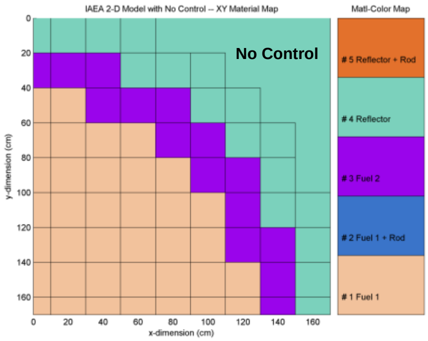

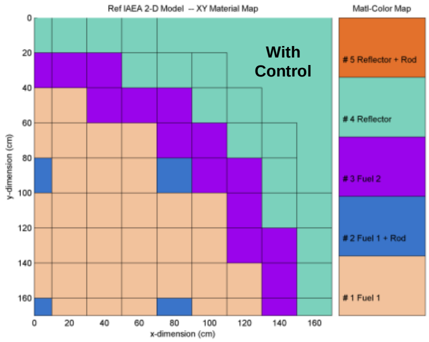

IAEA PWR Benchmark (cont.)

The figures below show the **X-directed group-dependent flux profiles** for the **control-out and control-in cases near the centerline** of the core (through $y \approx 169$ cm).

Both figures show a **peak in the thermal flux just after the core-reflector interface**.

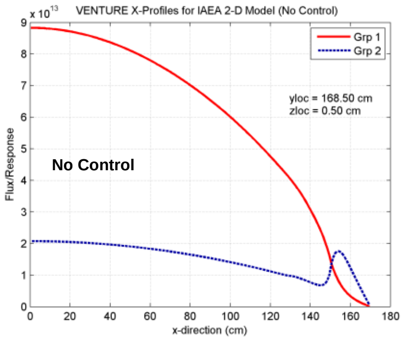

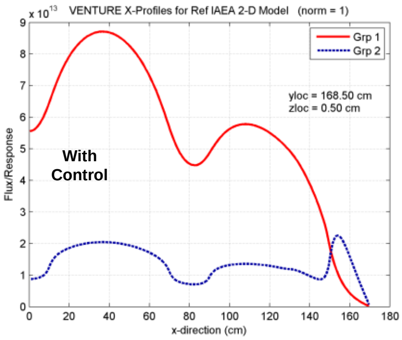

IAEA PWR Benchmark (cont.)

This buildup of thermal neutrons is due to the change in material properties at the interface, where the thermal absorption in the reflector is significantly lower than in the core.

Thus, the fast fission neutrons slowing down in this region tend to increase the thermal neutron flux and produce a very distinctive peak in the thermal flux profile.

Also, for the control vs. no control cases, we see that, in the vicinity of the poisoned assemblies, there are large depressions in both the fast and thermal flux profiles.

Here the large thermal absorption rate causes a reduction in the thermal flux and, in turn, this reduces the fission rate near these assemblies, which causes the depression in the fast flux.

IAEA PWR Benchmark (cont.)

Also, although the flux depressions just outside the controlled assemblies are still observable (see below), they are significantly reduced relative to the flux profiles directly through the controlled assemblies...

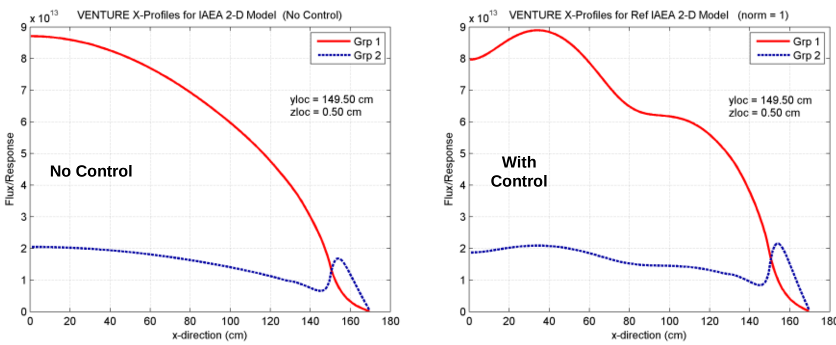

IAEA PWR Benchmark (cont.)

No Control

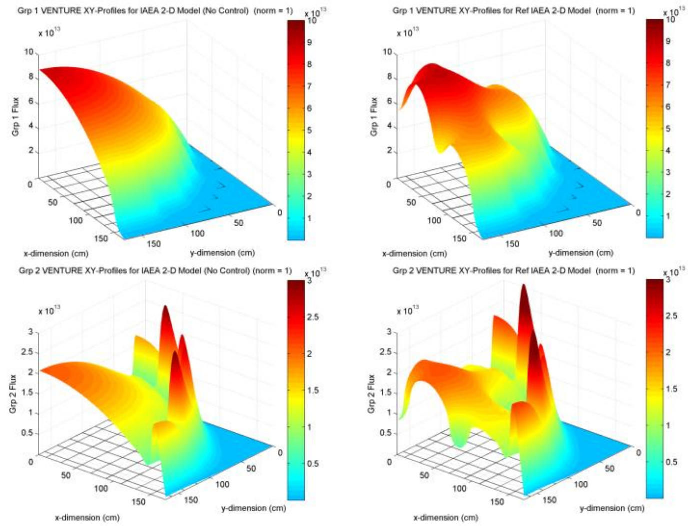

With Control

UMass-Lowell Research Reactor

The UMLRR is a 1 MW_{th} pool-type research reactor that serves as a teaching and training center and as a neutron and gamma source for a variety of material irradiation studies.

The facility was converted from the use of HEU fuel to LEU fuel in August 2000 and a new large-volume fast neutron irradiation (FNI) facility was designed and installed in early 2002.

To support these design efforts, a series of 2-D and/or 3-D models within VENTURE and DORT were developed and used to design the new configurations and to help analyze the actual as-built systems.

Here we illustrate some of the keys results…

UMass-Lowell Research Reactor (cont.)

The UMLRR fuel assembly contains 16 fuel plates and two dummy aluminum plates equally spaced within two grooved Al side plates (the sketch is rotated 90º relative to the arrangement in the core).

The reference design for the initial LEU core contained 19 full and 2 partial fuel assemblies in the arrangement shown (a partial element has the same geometry with half the U235 fuel loading).

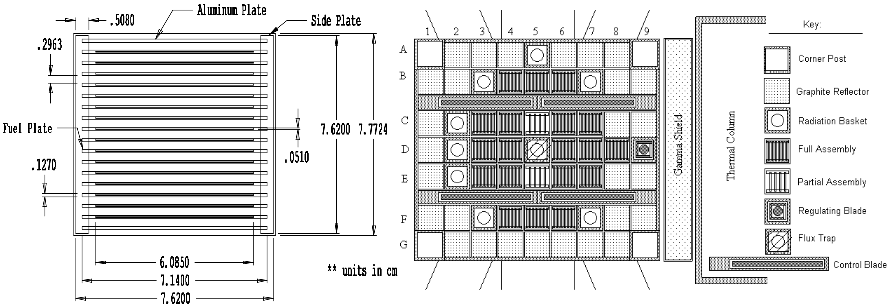

UMass-Lowell Research Reactor (cont.)

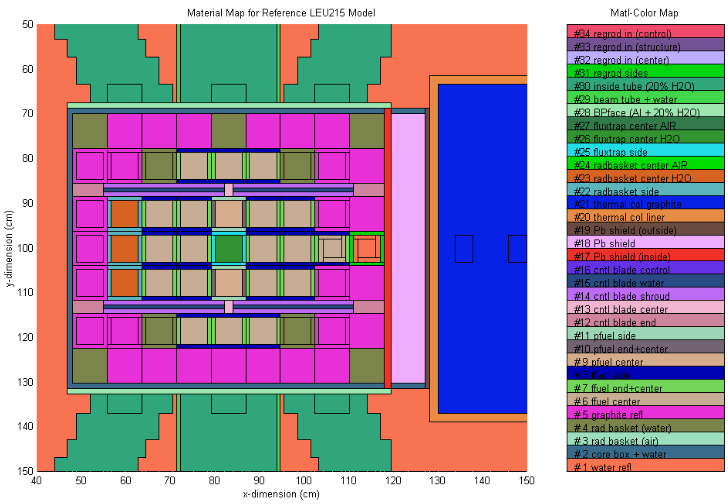

UMass-Lowell Research Reactor (cont.)

The geometry details associated with the assembly design and element configuration are important, since the changes in the macroscopic cross sections between individual regions give rise to much of the detailed structure seen in the resultant flux and power density plots (see next few slides after the discussion).

For example, the three large peaks in the thermal flux in the X-directed flux profiles are due to the radiation basket (RB) on the left, the central flux trap (FT) assembly, and the regulating blade region (in its control-out configuration) on the right.

The smaller intermediate peaks -- one on the left of the flux trap and two on the right side of the FT assembly -- are due to the dummy aluminum plates and unheated coolant channels on each side of the fuel assembly.

UMass-Lowell Research Reactor (cont.)

These water and aluminum regions act as small reflector zones where the thermal flux peaks due to the slowing down of the fast neutrons from the nearby fuel regions.

Similar behavior is also apparent in the Y-directed thermal flux profile, where the flux trap and the two water-filled control blade channels account for the three large flux peaks in this figure.

Also notice that the localized peak on the left side of the Y-directed thermal flux distribution is due to the water-filled radiation basket, and the smaller broader thermal flux peak on the right side of the model is due to the graphite reflector block (graphite has a much larger diffusion length than water and, therefore, the reflector peaks are usually not as large in graphite relative to water).

UMass-Lowell Research Reactor (cont.)

Concerning the fast flux distributions, much of the above discussion is also appropriate if we remember that the fast neutrons are born in the fuel regions and simply slow down to thermal in the non-fuel locations.

Thus, we would expect the fast flux to peak in the fuel and dip in the water and graphite non-fuel zones -- as observed in the plots…

The power density distribution is also as expected. Here, since most of the fissions are at thermal energies, the power density follows the thermal flux distributions in the fuel fairly closely.

Thus, we see that the power density peaks occur on the edges of the fuel assemblies because of the thermal flux peaks in the neighboring water regions.

Thus, everything here is as expected from basic theory…

UMass-Lowell Research Reactor (cont.)

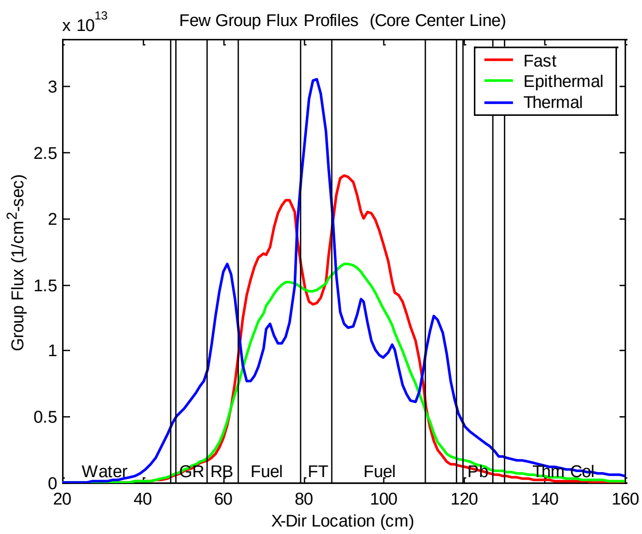

UMass-Lowell Research Reactor (cont.)

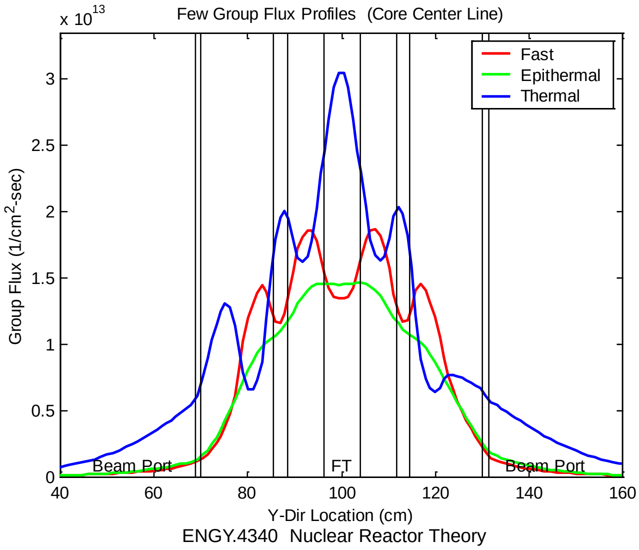

ENGY.4340 Nuclear Reactor Theory
Lesson 9: The Critical Reactor IV

(Oct. 2016)

UMass-Lowell Research Reactor (cont.)

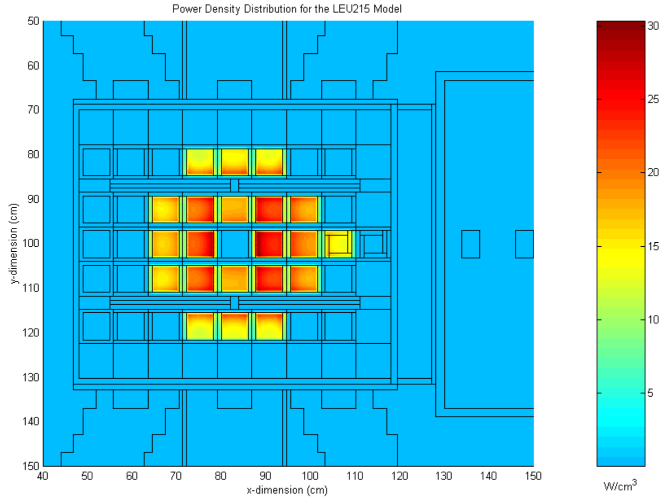

ENGY.4340 Nuclear Reactor Theory
Lesson 9: The Critical Reactor IV

(Oct. 2016)

UMass-Lowell Research Reactor (cont.)

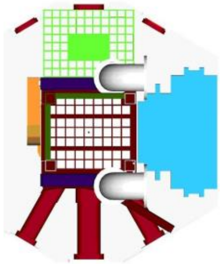

As a **final modeling example**, a series of pictures, diagrams, and modeling results associated with the **design and analysis of the fast neutron irradiator (FNI)** within the UMLRR are given here.

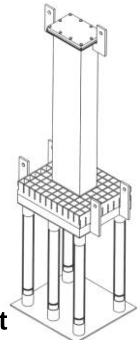

The **purpose of this experimental facility** is to provide an **easily accessible large-volume irradiation facility** that has a **relatively uniform fast flux ≥ 10^{11} n/cm^2-s over a 1 ft^2 area** parallel to the side of the core, that **minimizes the thermal neutron fluence rate and gamma dose to the extent possible**, and that has a **maximum reactivity effect below the limit for movable experiments** within the UMLRR (so that samples can be inserted/removed during full power operation).

UMass-Lowell Research Reactor (cont.)

side view

top view

aluminum collar

sample canister

UMass-Lowell Research Reactor (cont.)

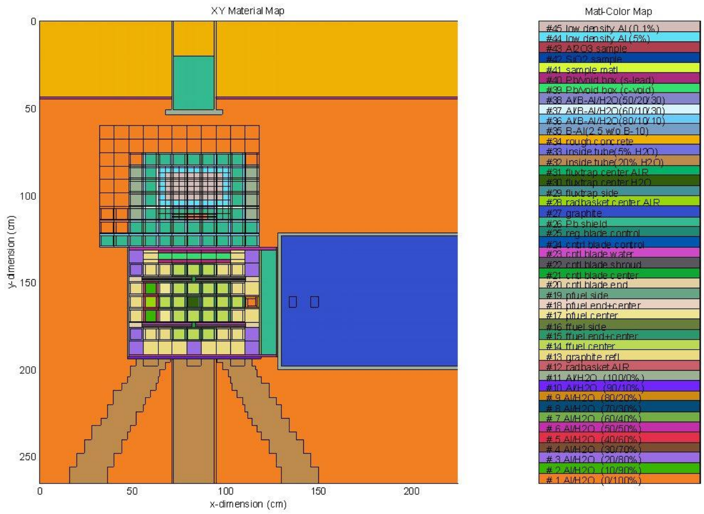

UMass-Lowell Research Reactor (cont.)

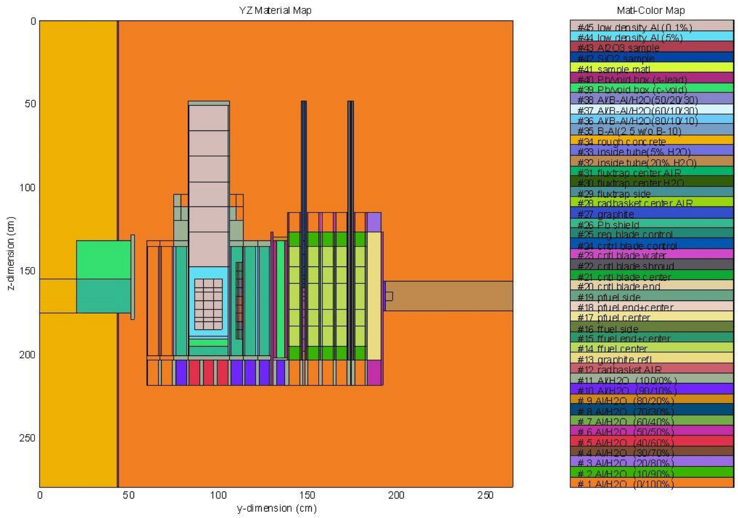

UMass-Lowell Research Reactor (cont.)

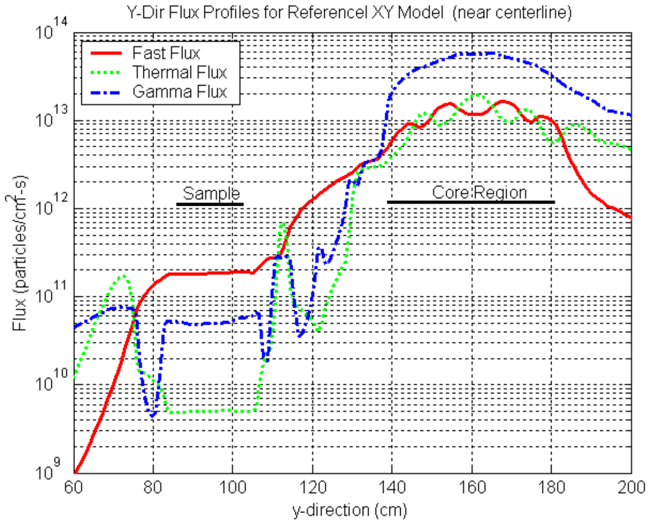

ENGY.4340 Nuclear Reactor Theory
Lesson 9: The Critical Reactor IV

(Oct. 2016)

UMass-Lowell Research Reactor (cont.)

Integral parameters for in-core location D2 and the new ex-core FNI facility.

Parameter of Interest	Radiation Basket D2	FNI Sample
Broad Group Fluxes (n/cm^2-sec)		
Fast Flux > 0.1 MeV	3.26E+12	1.83E+11
Epithermal Flux	3.42E+12	2.45E+11
Thermal Flux < 1 eV	1.14E+13	4.85E+09
Total Neutron Flux	1.81E+13	4.33E+11
Total Gamma Flux	2.95E+13	5.05E+10
Additional Fast Flux Characterization		
Fast Flux > 1 MeV	1.72E+12	5.08E+10
Fast Flux > 0.01 MeV	4.02E+12	2.55E+11
1 MeV Equiv. Flux	3.08E+12	1.39E+11
RDF	0.77	0.55
Energy Deposition Rates (Krad/hr)		
Neutrons in Air	2.58E+04	1.38E+02
Neutrons in Silicon	9.37E+02	3.20E+01
Gammas in Air	3.50E+04	4.40E+01
Gammas in Silicon	3.74E+04	4.62E+01

ENGY.4340 Nuclear Reactor Theory
Lesson 9: The Critical Reactor IV

(Oct. 2016)

UMass-Lowell Research Reactor (cont.)

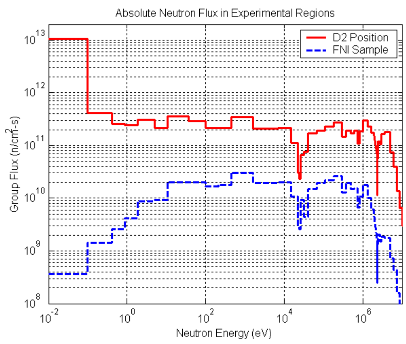

absolute neutron flux

Neutron Spectra in FNI vs. D2 Location

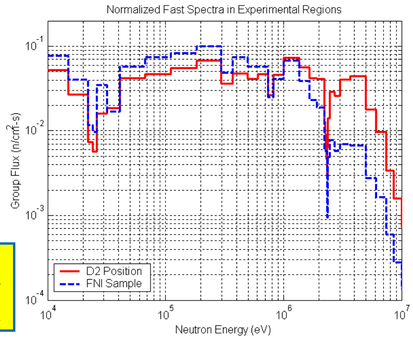

normalized high-energy neutron flux

Lesson 9 Summary

In this Lesson we have briefly discussed the following subjects:

The basic concepts of spatial and resonance self shielding.

How the lumping of the fuel into a heterogeneous geometry affects the thermal utilization and resonance escape probability.

How to create equivalent homogeneous regions that properly account for the heterogeneous detail in real geometries .

The nonlinear coupling that exists between the core physics problem and the temperature and flow distributions within a reactor.

The importance of the power peaking factors in various reactor geometries.

Lesson 9 Summary (cont.)

The existence of the peak in the thermal flux that is usually observed just beyond the core-reflector interface in most thermal systems.

The observed behavior in both the fast and thermal flux profiles in and near control rod locations in a typical thermal system.

Some of the fine structure in the observed flux profiles within the UMLRR…